Bone marrow-specific caspase-1/11 deficiency inhibits atherosclerosis development in Ldlr(-/-) mice

the FEBS Journal

Bone marrow-specific caspase-1/11 deficiency inhibits atherosclerosis development in *Ldlr*$^{-/-}$ mice

Tim Hendrikx[1,†], Mike L. J. Jeurissen[1,†], Patrick J. van Gorp[1], Marion J. Gijbels[1,2], Sofie M. A. Walenbergh[1], Tom Houben[1], Rick van Gorp[1], Chantal C. Pöttgens[1], Rinke Stienstra[3,4], Mihai G. Netea[3], Marten H. Hofker[5], Marjo M. P. C. Donners[1] and Ronit Shiri-Sverdlov[1]

1 Departments of Molecular Genetics and Pathology, School of Nutrition and Translational Research in Metabolism (NUTRIM) and School for Cardiovascular Diseases, University of Maastricht, The Netherlands
2 Departments of Medical Biochemistry and Experimental Vascular Biology, Academic Medical Center, University of Amsterdam, The Netherlands
3 Department of Medicine, Radboud University Nijmegen Medical Centre, The Netherlands
4 Department of Human Nutrition, Wageningen University,The Netherlands
5 Department of Pathology and Medical Biology, Molecular Genetics, Medical Biology Section, University of Groningen, University Medical Center Groningen, The Netherlands

Keywords
atherosclerosis; cardiovascular diseases; caspase-1/11; inflammasome; macrophage

Correspondence
R. Shiri-Sverdlov, Department of Molecular Genetics, Maastricht University, PO Box 616, 6200 MD Maastricht, The Netherlands
Fax: +31 43 388 4574
Tel: +31 43 388 1746
E-mail: r.sverdlov@maastrichtuniversity.nl

[†]These authors contributed equally to this work

(Received 17 July 2014, revised 19 February 2015, accepted 16 March 2015)

doi:10.1111/febs.13279

Recent investigations have suggested that inflammasome activation plays an important role during atherosclerosis. Upon activation, the inflammasome induces processing and release of pro-inflammatory cytokines interleukin 1β (IL-1β) and interleukin 18 (IL-18) via activation of caspase-1/11. Previously, it was shown that complete caspase-1 deficiency is protective against atherosclerosis development. However, while macrophages are the main inflammatory cells involved in atherosclerosis, the exact role of macrophage-specific caspase-1/11 activation during development of cardiovascular disease has never been investigated. We hypothesized that hematopoietic caspase-1/11 deficiency leads to reduced atherosclerosis development. To investigate the specific contribution of hematopoietic caspase-1/11 activation to atherosclerosis development, *Ldlr*$^{-/-}$ mice received a transplant (tp) of wild-type (WT) or caspase-1/11$^{-/-}$ bone marrow, to create WT-tp mice and caspase-1/11$^{-/-}$-tp mice, and fed a high-fat, high-cholesterol diet for 12 weeks. Our results showed an increase in anti-inflammatory blood leukocytes in caspase-1/11$^{-/-}$-tp mice compared with WT-tp mice, as indicated by a decreased level of Ly6C^{high} monocytes and an increased level of Ly6C^{low} monocytes. In line with our hypothesis, hematopoietic deletion of caspase-1/11 resulted in a strong reduction in atherosclerotic plaque size. Furthermore, necrotic core content was dramatically decreased in caspase-1/11$^{-/-}$-tp mice. Our data indicate that hematopoietic caspase-1/11 activation is involved in vascular inflammation and atherosclerosis, and plays an important role in cardiovascular disease progression.

Abbreviations
BMDMs, bone marrow-derived macrophages; FLICA, fluorescent-labeled inhibitors of caspases; HFD, high-fat, high-cholesterol diet; IL, interleukin; TNF, tumor necrosis factor.

Introduction

Atherosclerosis is one of the leading causes of death worldwide. The main characteristic of atherosclerosis is the development of plaques in the vessel wall due to accumulation of lipid-laden macrophages (foam cells). Although the exact mechanisms that drive atherosclerosis are complex and still not fully understood, inflammation and cell death are known to play a pivotal role [1]. Recent studies have indicated the involvement of inflammasomes in progression of atherosclerosis [2–4]. Phagocytosis of oxidized low-density lipoproteins, the most important risk factor for atherosclerosis, by macrophages was shown to activate the NOD-like receptor family, pyrin domain containing 3 (NLRP3) inflammasome [5]. Furthermore, cholesterol crystals, which are characteristic of advanced plaques, were found to activate NLRP3 inflammasomes, thereby triggering the inflammatory response during atherosclerosis [6].

Upon activation by various stimuli, the inflammasome induces the processing and release of the pro-inflammatory cytokines interleukin 1β (IL-1β) and interleukin 18 (IL-18) via caspase-1. Whereas caspase-1 is involved in the canonical pathway of inflammasome activation, caspase-11 was found to trigger caspase-1-dependent IL-1β and IL-18 release in response to non-canonical inflammasome activators [7,8]. Previously, complete caspase-1 deficiency was described as protective against atherosclerosis development, as reduced plaque size was observed in *ApoE*$^{-/-}$ *caspase-1*$^{-/-}$ mice compared with *ApoE*$^{-/-}$ mice receiving a Western type diet [9,10]. Furthermore, the reduction in plaque area was associated with fewer macrophages and vascular smooth muscle cells present in the plaques, and lower levels of the interleukins IL-1β and IL-6, plus the chemokine (C-C motif) ligand 2 (CCL2) and the cytokine tumor necrosis factor α (TNFα), in the plasma of double knockout mice [10]. However, so far, the specific contribution of hematopoietic caspase-1/11 activation to atherosclerosis development has not been established. We hypothesized that hematopoietic caspase-1/11 deficiency leads to reduced atherosclerosis development.

To test this hypothesis, bone marrow cells from wild-type (WT) donor mice or mice lacking caspase-1/11 were transferred into lethally irradiated hyperlipidemic *Ldlr*$^{-/-}$ recipient mice to create WT-tp mice and caspase-1/11$^{-/-}$-tp mice that were then put on a high-fat, high-cholesterol diet (HFD) for 12 weeks. In line with our hypothesis, hematopoietic deletion of caspase-1/11 resulted in a substantial reduction in atherosclerotic plaque size. Additionally, caspase-1/11$^{-/-}$-tp mice showed reduced cell death in the plaque area compared with controls. Our data indicate that hematopoietic caspase-1/11 activation plays an important role in vascular inflammation and atherosclerosis.

Results

Increased anti-inflammatory blood leukocyte profile in caspase-1/11$^{-/-}$-tp mice compared with WT-tp mice after 12 weeks of a high-fat, high-cholesterol diet

As shown previously, after 12 weeks of HFD, no differences were observed in the levels of triglycerides (2.372 ± 0.2378 versus 1.938 ± 0.1937 mM), free fatty acids (1.120 ± 0.084 versus 1.121 ± 0.099 mM) or cholesterol (40.14 ± 3.88 versus 34.32 ± 2.69 mM) in the plasma of WT-tp and caspase1/11$^{-/-}$-tp mice [11].

To elucidate the systemic effects of hematopoietic caspase-1/11 deficiency, fluorescence-activated cell sorting was performed to characterize the blood leukocyte profile of WT-tp and caspase-1/11$^{-/-}$-tp mice after 12 weeks of chow or HFD. There were no differences in the numbers of leukocytes between WT-tp and caspase-1/11$^{-/-}$-tp mice (Fig. 1A). Interestingly, when examining leukocyte subsets, the population of total monocytes was found to increase 1.6-fold in caspase-1/11$^{-/-}$-tp mice compared with WT-tp mice receiving HFD, but no difference was observed between the groups receiving chow versus HFD (Fig. 1B). Monocytes, which are precursors of macrophages, have various monocyte sub-populations with diverse functions, represented by the pro-inflammatory Ly6C^{high} monocyte population and the residential Ly6C^{low} monocyte population. In caspase-1/11$^{-/-}$-tp mice, the level of pro-inflammatory Ly6C^{high} monocytes decreased upon chow and HFD feeding compared with WT-tp mice (Fig. 1C). Further, the level of Ly6C^{low} monocytes dramatically increased in caspase-1/11$^{-/-}$-tp mice receiving HFD compared with WT-tp mice (Fig. 1D). These data indicate that hematopoietic deletion of caspase-1/11 results in reduced systemic inflammation after HFD.

To further define the inflammatory status of the experimental groups, plasma protein levels of the inflammatory cytokines CCL2, IL-12, TNFα, IL-6, IL-10 and interferon γ were measured. Protein levels of CCL2 were significantly reduced in caspase-1/11$^{-/-}$-tp mice compared with WT-tp mice (Fig. 2A), but no differences in the protein levels of other inflammatory cytokines were observed (Fig. 2B–F). These data indicate that hematopoietic caspase-1/11 deficiency results

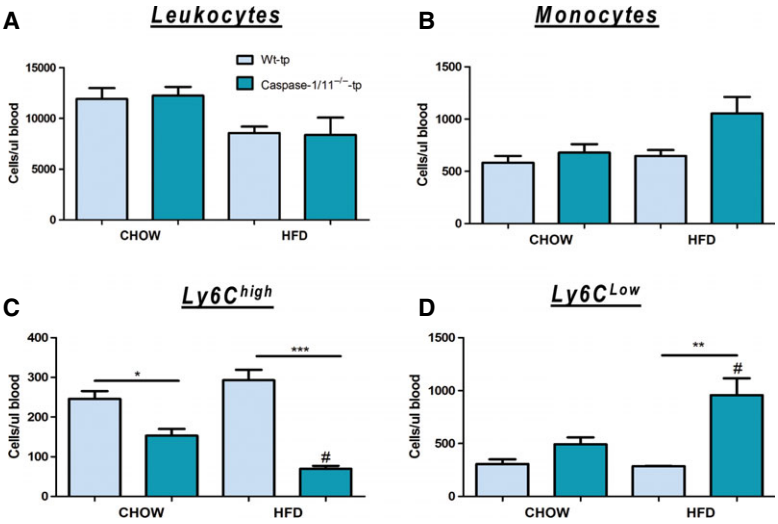

Fig. 1. Blood leukocyte profile. (A, B) Populations of leukocytes (A) and monocytes (B) after 12 weeks on chow or HFD in WT-tp and caspase-1/11$^{-/-}$-tp mice. (C, D) Sub-populations of Ly6C^{high} monocytes (C) and Ly6C^{low} monocytes (D) in the blood of WT-tp and caspase-1/11$^{-/-}$-tp mice receiving chow or HFD for 12 weeks. Values are means ± SEM. Asterisks indicate values that are statistically significantly different between WT-tp and caspase-1/11$^{-/-}$-tp (*$P < 0.05$, **$P < 0.01$, ***$P < 0.001$). The hash symbols (#) indicate values that are statistically significantly different between mice receiving chow and those receiving HFD ($P < 0.05$).

in reduced production of CCL2, thereby potentially leading to less atherosclerosis.

Hematopoietic caspase-1/11 deficiency leads to a substantial reduction in atherosclerotic plaque size and affects plaque development

To examine the effect of hematopoietic caspase-1/11 deficiency on atherosclerosis development, we analyzed histological sections of the aortic root of WT-tp and caspase-1/11$^{-/-}$-tp mice receiving HFD. The aortic roots were stained with toluidine blue to determine plaque size (Fig. 3A). Caspase-1/11$^{-/-}$-tp mice showed a significant (1.5-fold) reduction in plaque size compared with WT-tp mice (Fig. 3B). Next, gene expression analysis for macrophage marker CD68 was performed in the aortic arches as the amount of macrophages present can give an indication of plaque size. A clear trend towards reduced expression of the CD68 gene in the aortic arch was observed in caspase-1/11$^{-/-}$-tp mice compared with WT-tp mice (Fig. 3C). However, it is important to bear in mind that atherosclerosis development in the aortic arch is slower than in the aortic roots [12,13], which may explain why CD68 expression was not reduced significantly. In addition, atherosclerotic lesions were classified as early, moderate and advanced lesions. This classification indicated that caspase-1/11$^{-/-}$-tp mice had more moderate and fewer advanced atherosclerotic lesions compared with WT-tp mice (Fig. 3D).

Analysis of expression of the IL-1β, IL-18 and IL-33 genes in the aortic arch did not reveal any differences between WT-tp and caspase-1/11$^{-/-}$-tp mice (Fig. 4A–C). Circulating protein levels of IL-1β and IL-18 in plasma samples of WT-tp and caspase-1/11$^{-/-}$-tp mice were determined. Whereas IL-1β was undetectable, IL-18 levels showed a trend towards reduced levels in caspase-1/11$^{-/-}$-tp compared with WT-tp mice (Fig. 4D, E, $P = 0.06$). Further, expression of the NLRP3 and absent in melanoma 2 (AIM2) genes, encoding two well-known components of the inflammasome, revealed no difference in the expression of these genes in the aortic arch of WT-tp and caspase-1/11$^{-/-}$-tp mice (Fig. 4F,G). Taken together, these data indicate that atherosclerotic plaque development is considerably reduced in hematopoietic caspase-1/11-deficient mice, and lack of the caspases does not affect other parts of the inflammasome.

Reduced necrotic core content in mice with hematopoietic deletion of caspase1/11

To determine the effects of hematopoietic deletion of caspase-1/11 on plaque phenotype, (immuno)histological staining for various aspects of atherosclerosis was performed. Although no changes were seen in the relative amount of monocytes/macrophages (data not shown), we observed a significant reduction in the absolute amount of monocytes/macrophages in caspase-1/11$^{-/-}$-tp mice compared with WT-tp mice (Fig. 5A). In contrast, no changes were seen in relative collagen deposition (Sirius Red, Fig. 5B) or foam cell formation (Fig. 5C). Interestingly, the relative amount of necrosis in the plaque area (as determined by necrotic core measurement) was significantly reduced (1.7-fold) in caspase-1/11$^{-/-}$-tp mice compared with WT-tp mice receiving HFD (Fig. 5D,E). These data indicate that hematopoietic deletion of caspase-1/11 affects plaque composition by reducing the necrotic core content.

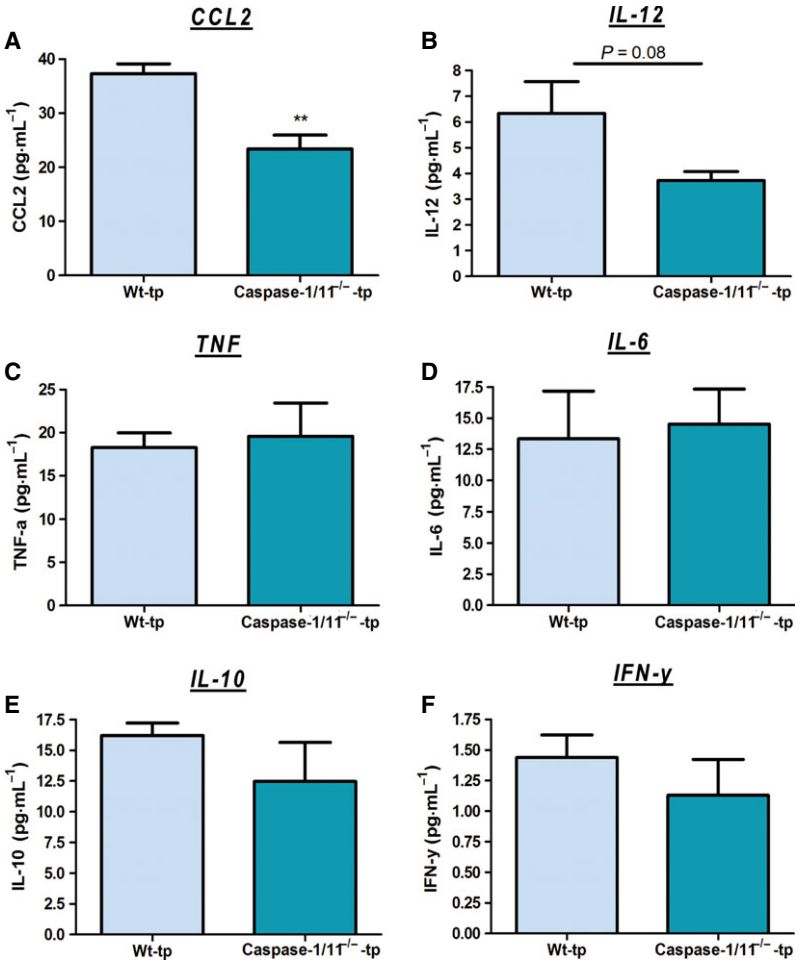

Fig. 2. Circulatory cytokine analysis. Plasma protein levels of the inflammatory cytokines CCL2 (A), IL-12 (B), tumor necrosis factor α (C), IL-6 (D), IL-10 (E) and interferon γ (F) after 12 weeks of HFD feeding in WT-tp and caspase-1/11$^{-/-}$-tp mice, respectively. Values are means ± SEM. Asterisks indicate a statistically significantly difference compared with WT-tp mice (**$P < 0.01$).

Hematopoietic deletion of caspase-1/11 reduces apoptosis, but not as a result of increased efficiency of efferocytosis

To determine whether hematopoietic deletion of caspase-1/11 also affects apoptosis, TUNEL staining on cryosections of the aortic root of WT-tp and caspase-1/11$^{-/-}$-tp mice was performed. As expected, TUNEL-positive stained area was significantly reduced (2.5-fold) in atherosclerotic plaques of caspase-1/11$^{-/-}$-tp mice compared with WT-tp mice (Fig. 6A,B). To investigate whether the reduction in apoptosis in the atherosclerotic plaques was due to an increase in the efficiency of clearance of apoptotic cell debris, an efferocytosis assay was performed. The capacity of bone marrow-derived macrophages (BMDMs) from WT and caspase-1/11$^{-/-}$ mice to take up apoptotic cells was analyzed in an *in vitro* assay. Despite the reduction in apoptosis seen in atherosclerotic plaques, no significant difference in efferocytosis was observed between WT and caspase-1/11$^{-/-}$ BMDMs (Fig. 6C). To investigate whether reduced cell death is partly related to pyroptosis (caspase-1-mediated cell death), expression of the caspase-1 gene in the aortic arch and caspase-1 activity in the aortic root in WT-tp and caspase-1/11$^{-/-}$-tp mice were assessed. A significant reduction in caspase-1 expression was found in the aortic arch in caspase-1/11$^{-/-}$-tp mice compared with WT-tp mice (Fig. 6D), but no difference in caspase-1 activity was observed (Fig. 6E).

Hematopoietic deletion of caspase-1/11 does not affect platelet activation

Infiltration of platelets into the plaque is aggravated by initiation of plaque rupture and formation of intra plaque hemorrhages inside these atherosclerotic lesions. Toluidine staining of slides of the aortic root of WT-tp and caspase-1/11$^{-/-}$-tp mice was performed to assess the presence of intra plaque hemorrhages. No intra plaque hemorrhages were identified in either WT-

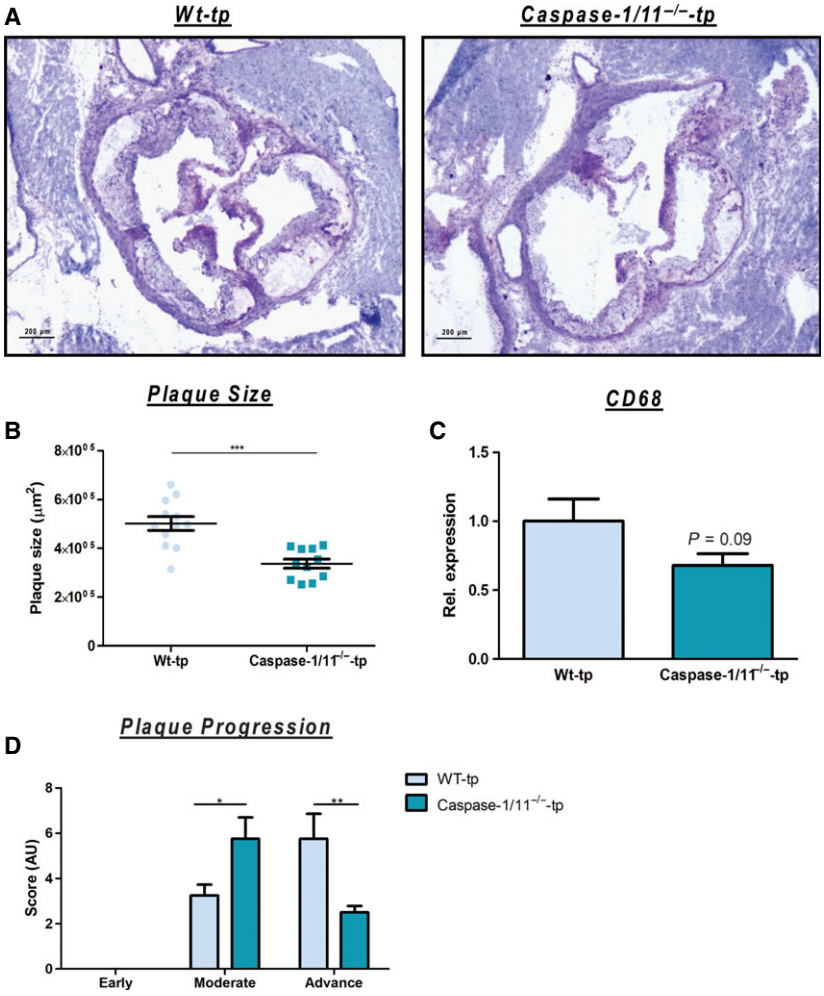

Fig. 3. Analysis of atherosclerotic plaque size. (A) Representative images of toluidine blue staining of aortic roots in WT-tp and caspase-1/11$^{-/-}$-tp mice, respectively. (B) Quantification of the total plaque size. (C) Expression of CD68 in the aortic arch of WT-tp and caspase-1/11$^{-/-}$-tp mice (n = 12 for WT-tp mice and n = 13 for caspase-1/11$^{-/-}$-tp mice). (D) Classification of atherosclerotic lesions in WT-tp and caspase-1/11$^{-/-}$-tp mice as early, moderate and advanced lesions. Values are means ± SEM, and are relative to values in WT-tp mice. Asterisks indicate values that are statistically significantly different from WT-tp (*P < 0.05, **P < 0.01, ***P < 0.001).

tp or caspase-1/11$^{-/-}$-tp mice (data not shown). In addition, May–Grünwald Giemsa staining was performed to assess the proportion of platelets inside the plaque. In line with previous data, staining revealed that no platelets were present in plaques of WT-tp and caspase-1/11$^{-/-}$-tp mice (data not shown). To determine whether platelet activation occurred in the atherosclerotic lesion, we performed gene expression analysis for platelet activation markers in the aortic arch the WT-tp and caspase-1/11$^{-/-}$-tp mice. The results showed no significant differences in the expression of C–C chemokine receptor type 2 (CCR2), C–C chemokine receptor type 5 (CCR5) and C–X–C chemokine receptor type 4 (CXCR4), C–C chemokine ligand type 5 (CCL5) and P-selectin between WT-tp and caspase-1/11$^{-/-}$-tp mice (Fig. 7A–E). While we cannot exclude the potential involvement of platelet activation, these data suggest that platelet activation is not a major mechanism associated with plaque development in these mice.

Discussion

Atherosclerosis is one of the major risk factors for developing the clinical complications of cardiovascular disease. Our aim was to investigate the role of hematopoietic caspase-1/11 activation during atherosclerosis development. We hypothesized that hematopoietic caspase-1/11 deficiency is protective against vascular inflammation, leading to reduced atherosclerosis. Here, we show that hematopoietic caspase-1/11 deficiency leads to a substantial reduction in atherosclerotic plaque size and necrotic core formation. Our data indicate that hematopoietic caspase-1/11 activation plays an important role in vascular inflammation and atherosclerosis.

Previously, inflammasomes were shown to contribute to the development of atherosclerosis, potentially via activation by cholesterol crystals [6,14]. Interestingly, cholesterol crystals were found to be present in atherosclerotic lesions, and were shown to induce

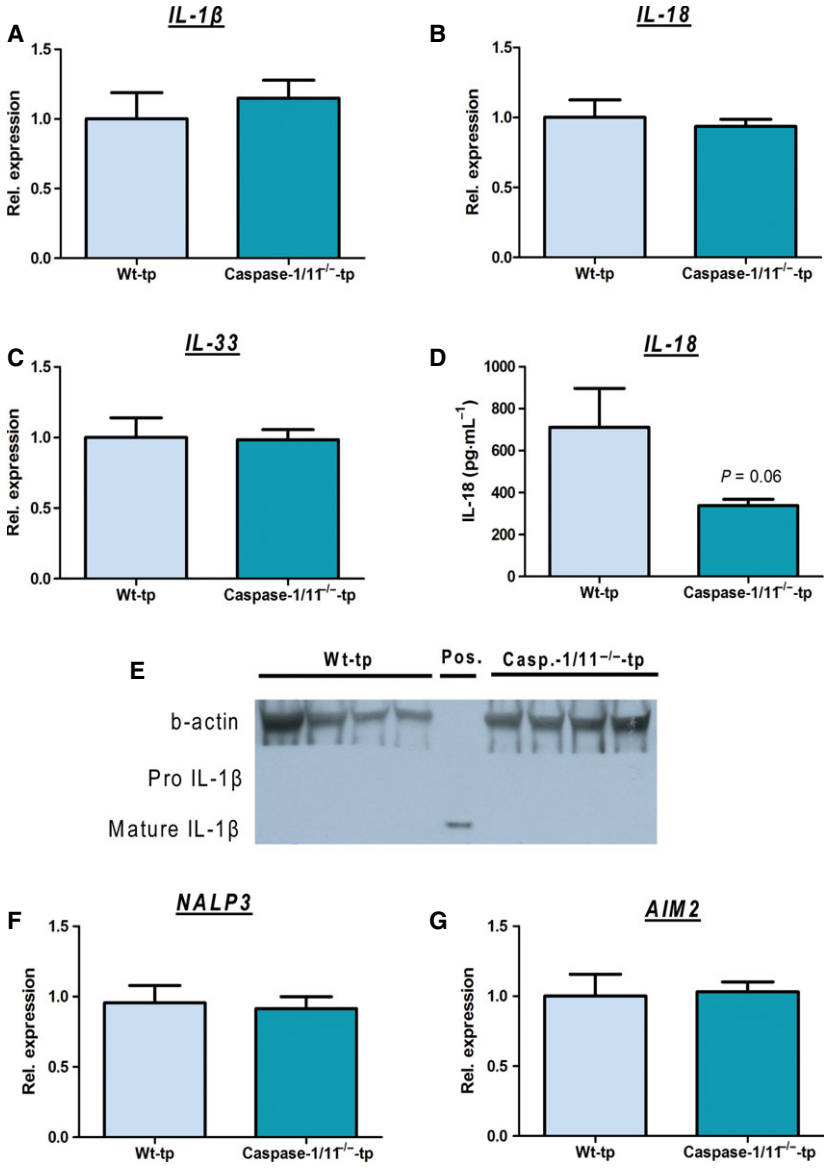

Fig. 4. Expression of inflammatory genes. (A–C) Expression of IL-1β (A), IL-18 (B) and IL-33 (C) in the aortic arch of WT-tp and caspase-1/11$^{-/-}$-tp mice after 12 weeks of HFD. (D) Plasma IL-18 protein levels in WT-tp and caspase-1/11$^{-/-}$-tp mice. (E) Western blot analysis of pro- and mature IL-1β levels. (F, G) Gene expression of NALP3 (F) and AIM2 (G) in WT-tp and caspase-1/11$^{-/-}$-tp mice. Values are means ± SEM, and are relative to values in WT-tp mice.

inflammasome activation in human macrophages [14]. More recently, it was found that the scavenger receptor CD36 coordinates ligands towards inflammasome activation, providing a potential mechanism for the role of inflammasomes in atherosclerosis [15]. The role of caspase-1 during atherosclerosis development hase been described previously [9,10,16]. Using *ApoE*$^{-/-}$ *caspase-1*$^{-/-}$ double knockout mouse models, it was shown that caspase-1 plays a critical role in vascular inflammation, and promotes atherosclerosis by enhancing inflammation in the lesion as reduced numbers of macrophages and vascular smooth muscle cells were found in the plaques compared with *ApoE*$^{-/-}$ mice [10,16]. Furthermore, *ApoE*$^{-/-}$ *caspase-1*$^{-/-}$ mice had significantly reduced plaque areas compared with controls, and lower plasma levels of inflammatory cytokines i.e. IL-1β, CCL2 and TNFα [10]. Despite these observations, one study claimed that atherosclerosis progresses independently of the inflammasome [16]. A possible explanation for the differences in the findings may be the different mouse models used to study atherosclerosis. Although both models are known to efficiently develop atherosclerotic lesions, *ApoE*$^{-/-}$ mice are generally more hypercholesterolemic and spontaneously develop atherosclerosis, whereas *Ldlr*$^{-/-}$ mice do not [16]. However, the specific role of caspase-1/11 in hematopoietic cells was not described in these studies. In the present study, we show that hematopoietic dele-

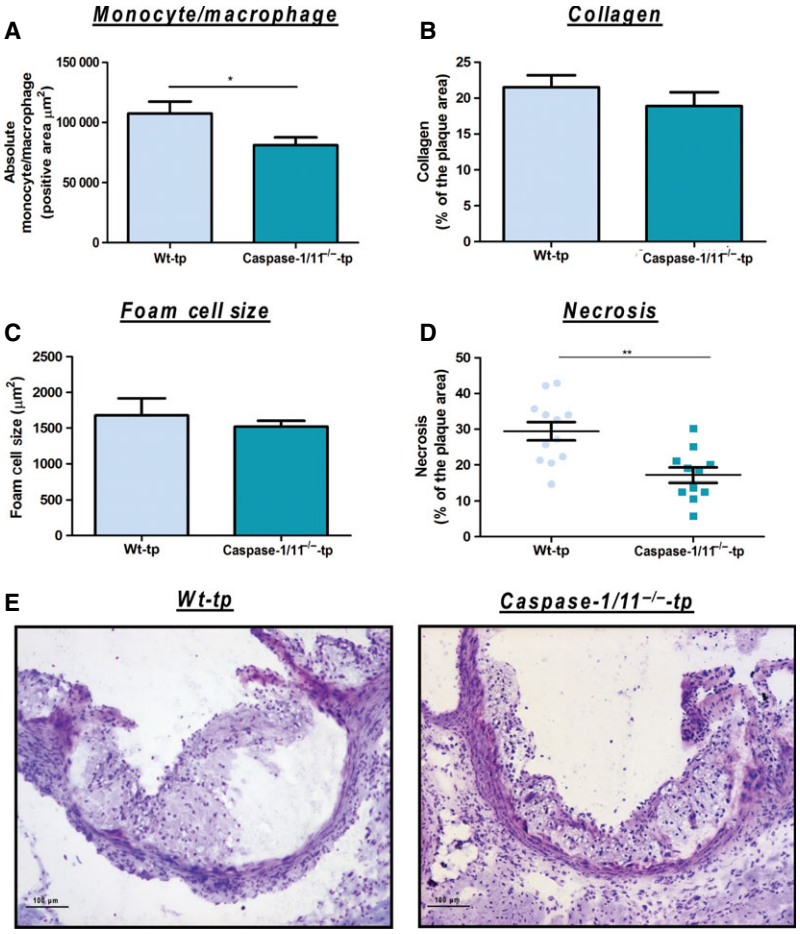

Fig. 5. Plaque phenotype analysis. (A–C) Quantification of (A) MOMA-2 staining for monocytes/macrophages (absolute), (B) Sirius Red staining for collagen deposition, and (C) foam cell formation in WT-tp and caspase-1/11$^{-/-}$-tp mice. (D, E) Quantification (D) and representative images (E) of necrosis in WT-tp and caspase-1/11$^{-/-}$-tp mice. Values are means ± SEM. Asterisks indicate values that are statistically significantly different from WT-tp (*$P < 0.05$, **$P < 0.01$).

tion of caspase-1/11 reduces atherosclerosis development, indicating that macrophage-specific inflammasome activation plays an important role in cardiovascular disease. In addition, we observed a significant change in the monocyte subsets in circulation. Ly6C^{high} monocytes are known to be inflammatory, and migrate to injured or infected sites [17,18]. On the other hand, Ly6C^{low} monocytes patrol the resting vasculature and participate in resolution of inflammation [19]. As Ly6C^{high} monocytes differentiate into cells that resemble M1 macrophages (pro-inflammatory), and cells derived from Ly6C^{low} monocytes exhibit M2 characteristics (anti-inflammatory), this may lead to a different macrophage phenotype within the plaque [19,20]. The mechanism by which caspase-1/11 affects the circulatory monocyte subsets is currently not understood. Potential mechanisms include altered conversion of inflammatory monocytes, increased survival of resident monocytes, or differences in monocyte trafficking. We showed that protein levels of CCL2 were significantly reduced in caspase-1/11$^{-/-}$-tp mice compared with WT-tp mice. CCL2 is a key chemokine that regulates migration and infiltration of monocytes/macrophages. Further, CCL2 was shown to be involved in atherosclerosis by regulating migration of monocytes from the bloodstream across the vascular endothelium [21]. In addition, it was shown that the higher the expression of either CCL2 or its receptor CCR2, the higher the likelihood of developing atherosclerosis in genetically modified animals [22]. Follow-up studies are required to further investigate the mechanisms by which caspase-1/11 modulates monocyte subsets in the circulation, as our data suggest that atherosclerosis development may be diminished by such modulation towards anti-inflammatory monocytes.

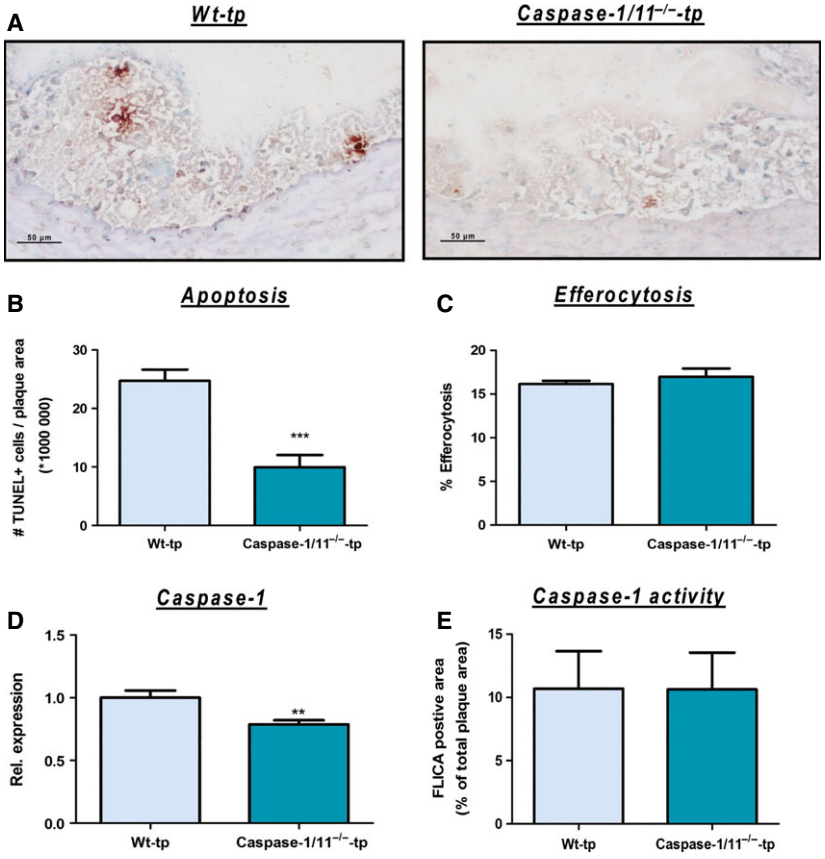

Fig. 6. TUNEL staining, efferocytosis analysis and analysis of expression of the caspase-1 gene and caspase-1 activity. (A) Representative images of TUNEL staining after 12 weeks of HFD feeding in WT-tp and caspase-1/11$^{-/-}$-tp mice. (B) Quantification of TUNEL staining for apoptosis. (C) *In vitro* efferocytosis assay of WT and caspase-1/11$^{-/-}$ BMDMs. (D) Expression of the caspase-1 gene in the aortic arch in WT-tp and caspase-1/11$^{-/-}$-tp mice. Values are means ± SEM, and are relative to values in WT-tp mice. (E) Quantification of caspase-1 activity (FLICA assay) in the aortic root of WT-tp and caspase-1/11$^{-/-}$-tp mice. Values are means ± SEM. Asterisks indicate values that are statistically significantly different from WT-tp receiving HFD (**$P < 0.01$, ***$P < 0.001$).

Although apoptosis is well documented in atherosclerosis, recent studies showed that pyroptosis also plays an important role in atherosclerosis and plaque stability [23,24]. Pyroptosis is a caspase-1-dependent apoptotic process characterized by the presence of inflammatory cytokines. In the present study, no change in caspase-1 activity was observed in caspase-1/11$^{-/-}$-tp mice compared with WT-tp mice. These data suggest that cell death occurred mainly via apoptosis and not via pyroptosis. Recent studies have shown that the chemokine CCL2 plays a major role in apoptotic processes in various diseases [25–27]. *In vitro*, it was shown that CCL2-primed macrophages are cytotoxic and enhance pro-apoptotic capacity [25]. These data are in line with our observation that CCL2 is reduced in the plasma of caspase-1/11$^{-/-}$-tp mice, and suggest that apoptotic cell death in atherosclerotic plaques of these mice is CCL2-dependent.

In conclusion, we have shown that hematopoietic caspase-1/11 contributes to atherosclerosis development. The mice used lacked caspase-11 in addition to caspase-1. Whereas caspase-1 is a key player in canonical inflammasome activation, caspase-11 has been found to be important in non-canonical inflammasome activation. The non-canonical caspase-11 inflammasome may interact with caspase-1 via the caspase recruitment domains [8]. Further, caspase-11, but not caspase-1, is a major sensor of lipopolysaccharides, and is mainly involved in inflammation driven by Gram-negative bacteria [7]. In addition, inflammasomes have been shown to control sterile low-grade inflammation independently of non-canonical caspase-11 activation [28]. As inflammasome activation by cholesterol crystals during atherosclerosis was shown to be caspase-1-dependent [14], it is most likely that caspase-11 plays a minor role in this process. Therefore, caspase-1 may be a promising target for the improvement of future therapy options.

Experimental procedures

Mice, diet and bone marrow transplantation

Mice were housed under standard conditions, and given unlimited access to food and water. Animal experiments were performed according to Dutch regulations, and approved by the Committee for Animal Welfare of Maastricht University. Female 10–12-week-old *Ldlr*$^{-/-}$ mice were lethally irradiated and transplanted with WT or caspase-1/11$^{-/-}$ bone marrow as previously described [29].

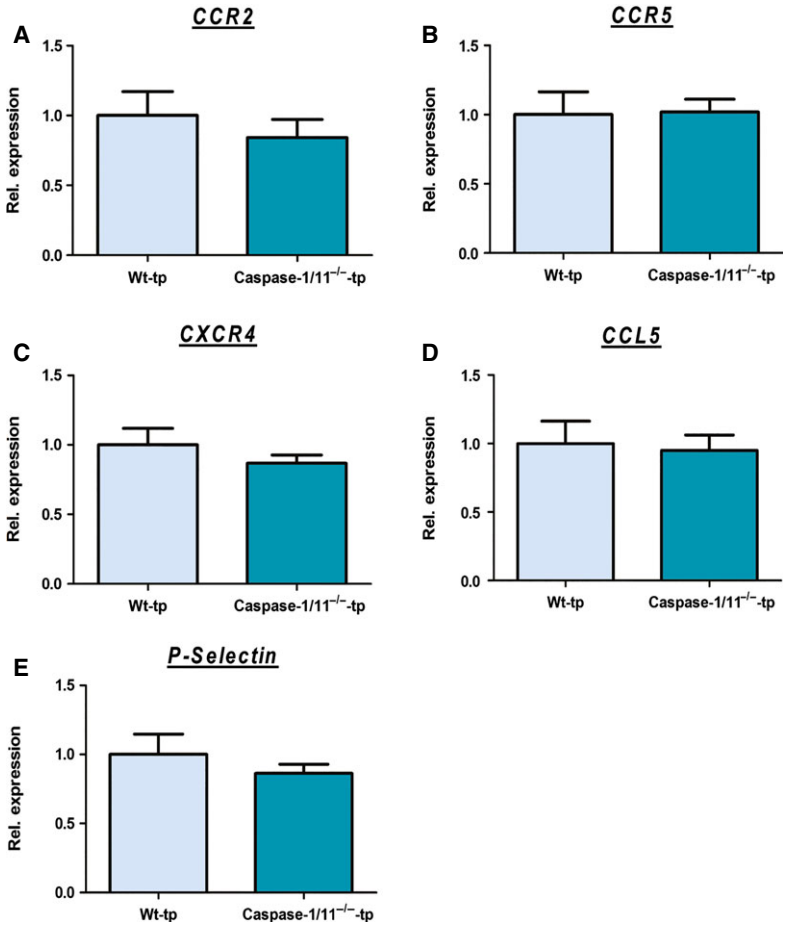

Fig. 7. Gene expression analysis for platelet activation markers. Expression of genes encoding CCR2 (A), CCR5 (B), CXCR4 (C), CCL5 (D) and P-selectin (E) in the aortic arch of WT-tp and caspase-1/11$^{-/-}$-tp mice after 12 weeks of HFD. Values are means ± SEM, and are relative to values in WT-tp mice.

Caspase-1/11$^{-/-}$ mice were a kind gift from Mihai Netea (Department of Medicine, Radboud University Nijmegen Medical Centre and Nijmegen Institute for Infection, Inflammation and Immunity, Nijmegen, The Netherlands). All mice were back-crossed with C57Bl/6J mice for 10 generations, and age-matched wild-type C57Bl/6J mice were used as controls throughout the experiments. Besides caspase-1, these mice are also deficient in caspase-11. The efficiency of bone marrow transplantation was approximately 98% (data not shown). After 9 weeks of recovery, mice were given HFD for 12 weeks ($n = 12$ for WT-tp mice; $n = 14$ for caspase-1/11$^{-/-}$-tp mice). The HFD contained 21% milk butter, 0.2% cholesterol, 46% carbohydrates and 17% casein. Collection of blood and tissue specimens, biochemical determination of plasma lipids, RNA isolation, cDNA synthesis and quantitative PCR were performed as described previously [30–33].

Histological analysis and morphological analysis

For histological analysis, cross-sections of aortic roots of WT-tp and caspase-1/11$^{-/-}$-tp mice were sectioned (7 μm) and collected on a series of 24 slides. For quantification of atherosclerotic plaque formation, slides were stained with toluidine blue for visualization of the atherosclerotic lesions inside the aortic root. Atherosclerosis development was determined as described previously [34]. Furthermore, lesions in atherosclerotic plaques were classified as early, moderate or advanced as described previously [35]. Monocyte/macrophage levels and collagen content in atherosclerotic plaques were assessed by immunohistochemistry using MOMA-2 (monocyte/ macrophage) and Sirius Red, respectively, according to standard protocols. Caspase-1 activity was measured in the aortic root of both WT-tp and caspase-1/11$^{-/-}$-tp mice using fluorescent-labeled inhibitors of caspases (FLICA). Sections were fixed and then stained for 2 h at room temperature using a fluorescent probe for active caspase-1 (FAM-FLICA™ caspase-1 kit; Bio-Rad, California, CA, USA). Caspase-1 activity is represented as the positive area for fluorescent-labeled inhibitors of caspases relative to the total plaque size.

Fluorescence-activated cell sorting

Blood was drawn from the tail vein of WT-tp and caspase-1/11$^{-/-}$-tp mice at week 12 of HFD. Staining was

performed using Trucount beads (BD Biosciences, San Jose, CA, USA) according to the manufacturer's instructions. In short, CD16/32 antibody (eBioscience, San Diego, CA, USA; (1:100)) was added to anti-coagulated whole blood to block the Fc-receptor and incubated for 10 min in the dark at room temperature (RT). All antibodies were diluted in FACS buffer (PBS, 0.1% BSA, 0.01% sodiumazide) and were then added to the blood, shaken gently and incubated for 20 min in the dark at RT. To lyse the red blood cells, erylysis solution (8.4 g NH_4Cl/0.84 g NaHCO solution in 1 L Milli-Q; 7.2–7.4 pH) was added and incubated for 15 min in the dark at RT. Samples were measured within 1 h by FACS (BD FACSCanto II flow cytometer). The following stainings were performed: Leukocytes: $CD45^+$, Monocytes: $Ly6G^-CD11b^+$ and the inflammatory status of the monocytes via $Lys6C^+$.

Cytokine analysis

The cytokine profile in pooled plasma samples of WT-tp and caspase-$1/11^{-/-}$-tp mice was determined using a cytometric bead array mouse inflammation kit (BD Biosciences) according to the manufacturer's instructions. Beads coated with specific capture antibodies for IL-6, IL-10, CCL2, interferon γ, TNFα and IL-12 were mixed together and incubated for 2 h with standard or test samples in the presence of a phycoerythrin-conjugated detection antibody. Concentrations of these cytokines were determined by measuring the mean fluorescence intensity using a BD FACSCalibur™ (BD Biosciences) and comparing them with a standard curve. IL-18 levels were determined using an ELISA kit (mouse IL-18/IL-1F4 ELISA; R&D Systems, Minneapolis, MN, USA) according to the manufacturer's instructions.

Western blotting

Pro- and mature IL-1β levels were measured via western blot analysis. The total protein concentration was measured using a Pierce® (Waltham, MA, USA) BCA protein assay. Equal amounts of protein (60 μg) were loaded on the gel. After SDS/PAGE, proteins were transferred on nitrocellulose membrane (Bio-Rad). The membrane was blocked with 4% non-fat dry milk for 1 h at room temperature. For detection, the membrane was incubated with an antibody against IL-1β (1 : 1000 dilution; Cell Signaling Technology, Danvers, MA, USA) overnight at 4 °C followed by 1 h of incubation with donkey anti-rabbit antibody at room temperature (Jackson Laboratories, Bar Harbor, ME, USA). Signal was detected on autoradiograms by enhanced chemoluminescence. β-actin was used as a housekeeping protein (diluted 1 : 100 000; MP Biomedicals, Santa Ana, CA, USA).

Efferocytosis assay

Bone marrow cells were isolated from the bones of the hind limbs of WT and caspase-$1/11^{-/-}$ mice. Cells were cultured for 8 days in RPMI-1640 cell culture medium supplemented with 10% fetal bovine serum, 1% Penicillin and Strep (P/S), 1% L-glutamine, 20 mM HEPES (GIBCO/Invitrogen, Breda, The Netherlands) and 20% L929 cell-conditioned medium containing Macrophage colony stimulating factor to stimulate differentiation into bone-marrow derived macrophages (BMDMs). BMDMs of WT and caspase-$1/11^{-/-}$ mice were seeded into a 24-well plate in quadruplicate (0.2×10^6 cells per well). Jurkat cells were labeled using Calcein-AM (1 $mg \cdot mL^{-1}$, 1 : 2000 dilution; Invitrogen) and incubated for 1 h at 37 °C. To induce apoptosis, Jurkat cells were exposed to UV light (UVS-26; Fisher Scientific (Waltham, MA, USA); 254 nm, 6 W bulb, 0.02 $J \cdot s^{-1} \cdot cm^{-2}$) for 15 min. After a 4 h recovery period, BMDMs of WT or caspase-$1/11^{-/-}$ mice were added to the apoptotic Jurkat cells for 45 min. After washing for 1 min at room temperature with medium, the amount of efferocytosis was determined by FACS analysis by measuring the percentage of macrophages that incorporated Jurkat cells that are positively labeled for cell death with Calcein-AM.

Statistical analysis

The data were analyzed using GRAPHPAD PRISM 4.0.3 (GraphPad Software Inc., La Jolla, CA, USA). An unpaired *t* test was performed to compare WT-tp and caspase-$1/11^{-/-}$-tp mice for each diet group. For FACS data, one-way ANOVA was performed with Tukey's multiple comparison test.

Acknowledgements

This research was performed within the framework of the Center for Translational Molecular Medicine (www.ctmm.nl), project PREDICCt (grant number 01C-104), and supported by the Dutch Heart Foundation, the Dutch Diabetes Research Foundation, the Dutch Kidney Foundation, Maag Lever Darm Stichting (WO 08-16, WO 11-35 and WO 09-46) and Vidi grant 016.126.327. M.G.N. was supported by a Vici grant from the Nederlandse Organisatie voor Wetenschappelijk Onderzoek (Netherlands Organization for Scientific Research).

Author contributions

T.H., M.L.J.J., P.J.v.G., M.J.G., S.M.A.W., T.H., R.v.G., C.C.P., M.H.H., M.M.P.C.D. and R.S.-S. planned the experiments, performed the experiments,

analyzed the data and wrote the paper. R.S. and M.G.N. contributed reagents or other essential material.

References

1 Libby P (2012) Inflammation in atherosclerosis. *Arterioscler Thromb Vasc Biol* **32**, 2045–2051.

2 Freigang S, Ampenberger F, Spohn G, Heer S, Shamshiev AT, Kisielow J, Hersberger M, Yamamoto M, Bachmann MF & Kopf M (2011) Nrf2 is essential for cholesterol crystal-induced inflammasome activation and exacerbation of atherosclerosis. *Eur J Immunol* **41**, 2040–2051.

3 Hansson GK & Klareskog L (2011) Pulling down the plug on atherosclerosis: cooling down the inflammasome. *Nat Med* **17**, 790–791.

4 Masters SL, Latz E & O'Neill LA (2011) The inflammasome in atherosclerosis and type 2 diabetes. *Sci Transl Med* **3**, 81 ps17.

5 Jiang Y, Wang M, Huang K, Zhang Z, Shao N, Zhang Y, Wang W & Wang S (2012) Oxidized low-density lipoprotein induces secretion of interleukin-1beta by macrophages via reactive oxygen species-dependent NLRP3 inflammasome activation. *Biochem Biophys Res Commun* **425**, 121–126.

6 Duewell P, Kono H, Rayner KJ, Sirois CM, Vladimer G, Bauernfeind FG, Abela GS, Franchi L, Nunez G, Schnurr M *et al.* (2010) NLRP3 inflammasomes are required for atherogenesis and activated by cholesterol crystals. *Nature* **464**, 1357–1361.

7 Kayagaki N, Warming S, Lamkanfi M, Vande Walle L, Louie S, Dong J, Newton K, Qu Y, Liu J, Heldens S *et al.* (2011) Non-canonical inflammasome activation targets caspase-11. *Nature* **479**, 117–121.

8 Wang S, Miura M, Jung YK, Zhu H, Li E & Yuan J (1998) Murine caspase–11, an ICE-interacting protease, is essential for the activation of ICE. *Cell* **92**, 501–509.

9 Gage J, Hasu M, Thabet M & Whitman SC (2012) Caspase–1 deficiency decreases atherosclerosis in apolipoprotein E-null mice. *Can J Cardiol* **28**, 222–229.

10 Usui F, Shirasuna K, Kimura H, Tatsumi K, Kawashima A, Karasawa T, Hida S, Sagara J, Taniguchi S & Takahashi M (2012) Critical role of caspase–1 in vascular inflammation and development of atherosclerosis in Western diet-fed apolipoprotein E-deficient mice. *Biochem Biophys Res Commun* **425**, 162–168.

11 Hendrikx T, Bieghs V, Walenbergh SM, van Gorp PJ, Verheyen F, Jeurissen ML, Steinbusch MM, Vaes N, Binder CJ, Koek GH *et al.* (2013) Macrophage specific caspase–1/11 deficiency protects against cholesterol crystallization and hepatic inflammation in hyperlipidemic mice. *PLoS One* **8**, e78792.

12 Ma Y, Wang W, Zhang J, Lu Y, Wu W, Yan H & Wang Y (2012) Hyperlipidemia and atherosclerotic lesion development in Ldlr-deficient mice on a long-term high-fat diet. *PLoS One* **7**, e35835.

13 Paigen B, Morrow A, Holmes PA, Mitchell D & Williams RA (1987) Quantitative assessment of atherosclerotic lesions in mice. *Atherosclerosis* **68**, 231–240.

14 Rajamaki K, Lappalainen J, Oorni K, Valimaki E, Matikainen S, Kovanen PT & Eklund KK (2010) Cholesterol crystals activate the NLRP3 inflammasome in human macrophages: a novel link between cholesterol metabolism and inflammation. *PLoS One* **5**, e11765.

15 Sheedy FJ, Grebe A, Rayner KJ, Kalantari P, Ramkhelawon B, Carpenter SB, Becker CE, Ediriweera HN, Mullick AE, Golenbock DT *et al.* (2013) CD36 coordinates NLRP3 inflammasome activation by facilitating intracellular nucleation of soluble ligands into particulate ligands in sterile inflammation. *Nat Immunol* **14**, 812–820.

16 Menu P, Pellegrin M, Aubert JF, Bouzourene K, Tardivel A, Mazzolai L & Tschopp J (2011) Atherosclerosis in ApoE-deficient mice progresses independently of the NLRP3 inflammasome. *Cell Death Dis* **2**, e137.

17 Swirski FK, Libby P, Aikawa E, Alcaide P, Luscinskas FW, Weissleder R & Pittet MJ (2007) Ly-6Chi monocytes dominate hypercholesterolemia-associated monocytosis and give rise to macrophages in atheromata. *J Clin Invest* **117**, 195–205.

18 Tacke F, Alvarez D, Kaplan TJ, Jakubzick C, Spanbroek R, Llodra J, Garin A, Liu J, Mack M, van Rooijen N *et al.* (2007) Monocyte subsets differentially employ CCR2, CCR5, and CX3CR1 to accumulate within atherosclerotic plaques. *J Clin Invest* **117**, 185–194.

19 Nahrendorf M, Swirski FK, Aikawa E, Stangenberg L, Wurdinger T, Figueiredo JL, Libby P, Weissleder R & Pittet MJ (2007) The healing myocardium sequentially mobilizes two monocyte subsets with divergent and complementary functions. *J Exp Med* **204**, 3037–3047.

20 Geissmann F, Manz MG, Jung S, Sieweke MH, Merad M & Ley K (2010) Development of monocytes, macrophages, and dendritic cells. *Science* **327**, 656–661.

21 Deshmane SL, Kremlev S, Amini S & Sawaya BE (2009) Monocyte chemoattractant protein-1 (MCP-1): an overview. *J Interferon Cytokine Res* **29**, 313–326.

22 Coll B, Alonso-Villaverde C & Joven J (2007) Monocyte chemoattractant protein-1 and atherosclerosis: is there room for an additional biomarker? *Clin Chim Acta* **383**, 21–29.

23 Chang W, Lin J, Dong J & Li D (2013) Pyroptosis: an inflammatory cell death implicates in atherosclerosis. *Med Hypotheses* **81**, 484–486.

24 Lin J, Shou X, Mao X, Dong J, Mohabeer N, Kushwaha KK, Wang L, Su Y, Fang H & Li D (2013) Oxidized low density lipoprotein induced caspase–1 mediated pyroptotic cell death in macrophages: implication in lesion instability? *PLoS One* **8**, e62148.
25 Wang Q, Ren J, Morgan S, Liu Z, Dou C & Liu B (2014) Monocyte chemoattractant protein-1 (MCP-1) regulates macrophage cytotoxicity in abdominal aortic aneurysm. *PLoS One* **9**, e92053.
26 Yang D, Elner SG, Chen X, Field MG, Petty HR & Elner VM (2011) MCP-1-activated monocytes induce apoptosis in human retinal pigment epithelium. *Invest Ophthalmol Vis Sci* **52**, 6026–6034.
27 Nam BY, Paeng J, Kim SH, Lee SH, Kim do H, Kang HY, Li JJ, Kwak SJ, Park JT, Yoo TH *et al.* (2012) The MCP-1/CCR2 axis in podocytes is involved in apoptosis induced by diabetic conditions. *Apoptosis* **17**, 1–13.
28 Youm YH, Grant RW, McCabe LR, Albarado DC, Nguyen KY, Ravussin A, Pistell P, Newman S, Carter R, Laque A *et al.* (2013) Canonical Nlrp3 inflammasome links systemic low-grade inflammation to functional decline in aging. *Cell Metab* **18**, 519–532.
29 Bieghs V, Wouters K, van Gorp PJ, Gijbels MJ, de Winther MP, Binder CJ, Lutjohann D, Febbraio M, Moore KJ, van Bilsen M *et al.* (2010) Role of scavenger receptor A and CD36 in diet-induced nonalcoholic steatohepatitis in hyperlipidemic mice. *Gastroenterology* **138**, 2477–2486.
30 Bieghs V, Hendrikx T, van Gorp PJ, Verheyen F, Guichot YD, Walenbergh SM, Jeurissen ML, Gijbels M, Rensen SS, Bast A *et al.* (2013) The cholesterol derivative 27-hydroxycholesterol reduces steatohepatitis in mice. *Gastroenterology* **144**, 167–178 e1.
31 Bieghs V, van Gorp PJ, Walenbergh SM, Gijbels MJ, Verheyen F, Buurman WA, Briles DE, Hofker MH, Binder CJ & Shiri-Sverdlov R (2012) Specific immunization strategies against oxidized low-density lipoprotein: a novel way to reduce nonalcoholic steatohepatitis in mice. *Hepatology* **56**, 894–903.
32 Bieghs V, Verheyen F, van Gorp PJ, Hendrikx T, Wouters K, Lutjohann D, Gijbels MJ, Febbraio M, Binder CJ, Hofker MH *et al.* (2012) Internalization of modified lipids by CD36 and SR-A leads to hepatic inflammation and lysosomal cholesterol storage in Kupffer cells. *PLoS One* **7**, e34378.
33 Wisse E, Braet F, Duimel H, Vreuls C, Koek G, Olde Damink SW, van den Broek MA, De Geest B, Dejong CH, Tateno C *et al.* (2010) Fixation methods for electron microscopy of human and other liver. *World J Gastroenterol* **16**, 2851–2866.
34 Kanters E, Pasparakis M, Gijbels MJ, Vergouwe MN, Partouns-Hendriks I, Fijneman RJ, Clausen BE, Forster I, Kockx MM, Rajewsky K *et al.* (2003) Inhibition of NF-kappaB activation in macrophages increases atherosclerosis in LDL receptor-deficient mice. *J Clin Invest* **112**, 1176–1185.
35 Donners MM, Wolfs IM, Stoger LJ, van der Vorst EP, Pottgens CC, Heymans S, Schroen B, Gijbels MJ & de Winther MP (2012) Hematopoietic miR155 deficiency enhances atherosclerosis and decreases plaque stability in hyperlipidemic mice. *PLoS One* **7**, e35877.